Electronic Supplementary Material (ESI) for Journal of Materials Chemistry A
This journal is © The Royal Society of Chemistry 2017

Visible-Light Responsive MOF Encapsulation of Noble-Metal-Sensitized Semiconductors for High-Performance Photoelectrochemical Water Splitting

Yibo Dou,[a,b] Jian Zhou,[b] Awu Zhou,[b] Jian-Rong Li,[a,b,*] and Zuoren Nie[a,*]

[a] *The Key Laboratory of Advanced Functional Materials, Ministry of Education, College of Materials Science and Engineering, Beijing University of Technology, Beijing 100124, P. R. China.*
E-mail: zrnie@bjut.edu.cn. Tel: +86-10-67391536

[b] *Beijing Key Laboratory for Green Catalysis and Separation and Department of Chemistry and Chemical Engineering, College of Environmental and Energy Engineering, Beijing University of Technology, Beijing 100124, P. R. China.*
E-mail: jrli@bjut.edu.cn. Tel: +86-10-67392332

The Relevant Theoretical Calculation

1. ***Calculation of the photoconversion efficiency (η) and incident-photon-to-current conversion efficiency (IPCE)***: The photoconversion efficiency was calculated using the following equation:[1]

$$\eta(\%) = Photocuurent\ density \times (1.23 - E_{appl\ vs.\ RHE}) / (light\ density) \times 100\% \quad (1)$$

For IPCE measurements, various wavelengths of monochromatic light were produced using a monochromator, and the resultant photocurrents were recorded at 0.6 V *vs*. SCE. IPCE was calculated using the following equation:

$$\text{IPCE}(\%) = 1240 \times Photocurrent\ density / (Wavelength \times photon\ \text{flux}) \quad (2)$$

2. ***Calculation of the band gaps (E_g) of the semiconductors*:** The E_g for pristine ZnO was calculated according to the following equation: [2]

$$(\alpha hv)^n = K(hv - E_g) \quad (3)$$

where α is the absorption coefficient, hv is the energy of the photon, and n represents the index that depends on the electronic transition of the semiconductor.

3. ***Calculation of the electrochemically active surface area (ECSA)*:** The ECSA for each system was estimated from the double-layer capacitance (C_{dl}). To obtain the double-layer charging *via* cyclic voltammetry (CV) curves, all currents were measured in the non-Faradaic potential region of 0.2 ~ 0.3 V *vs*. SCE at multiple scan rates of 10, 50, 100, 150, and 200 mV s^{-1}.[3-5] The anodic (I_a) and cathodic (I_c) charging currents in the middle of the potential window of the corresponding CV curves were plotted against the scan rate, and the linear slope was twice the values of C_{dl}. The ECSA was calculated from C_{dl} according to the following equation:

$$ECSA = C_{dl} / C_s \quad (4)$$

where C_s is the specific capacitance of the sample or the capacitance of an atomically smooth planar surface of the material per unit area under identical electrolyte conditions.[4,5] However, it is not practical for most electrocatalytic systems to utilize the smooth planar surface of a catalyst to measure C_s. The commonly used C_s values are those measured for a variety of metal electrodes in acidic and alkaline solutions. Unfortunately, the electrolyte used in this configuration is a neutral Na_2SO_4 aqueous solution, which has not been used for the measurement of C_s. Considering the test conditions in this system,

the C_s of an FTO substrate in a 0.5 M Na_2SO_4 electrolyte was measured for the calculation of ECSA.[4]

4. ***Calculation of the charge-separation and charge-injection efficiencies*:** The observed PEC photocurrent density (J_{PEC}) arising from water oxidation was determined by following equation: [5]

$$J_{PEC} = J_{abs} \times \phi_{sep} \times \phi_{inj} \quad (5)$$

where J_{abs} is the photocurrent density based on complete photon conversion efficiency, ϕ_{sep} is the charge separation yield of the photogenerated carriers that migrate to the electrode/electrolyte interface, and ϕ_{inj} is the charge-injection yield from the electrode to the electrolyte, which represents the efficiency of the water-oxidation process. A hole scavenger is added into the electrolyte to suppress surface recombination and inhibit the holes from reaching the surface in the water-oxidation process (charge injection), owing to its fast hole-capture kinetics, which results in a charge-injection efficiency of 100%.[6-8] Herein, we chose a widely used hole scavenger Na_2SO_3 for this investigation.[9] Moreover, the charge separation and charge injection can be calculated according to the following equations:

$$\phi_{sep} = J_{Na_2SO_3} / J_{abs} \quad (6)$$

$$\phi_{inj} = J_{H_2O} / J_{Na_2SO_3} \quad (7)$$

ZnO is the semiconductor photocatalyst in these four photoanodes. In addition, J_{abs} for these photoanodes was calculated to be 2.04 mA cm^{-2} under irradiation with the Xe lamp (100 mW cm^{-2}).[7,9]

Additional Figures and Tables

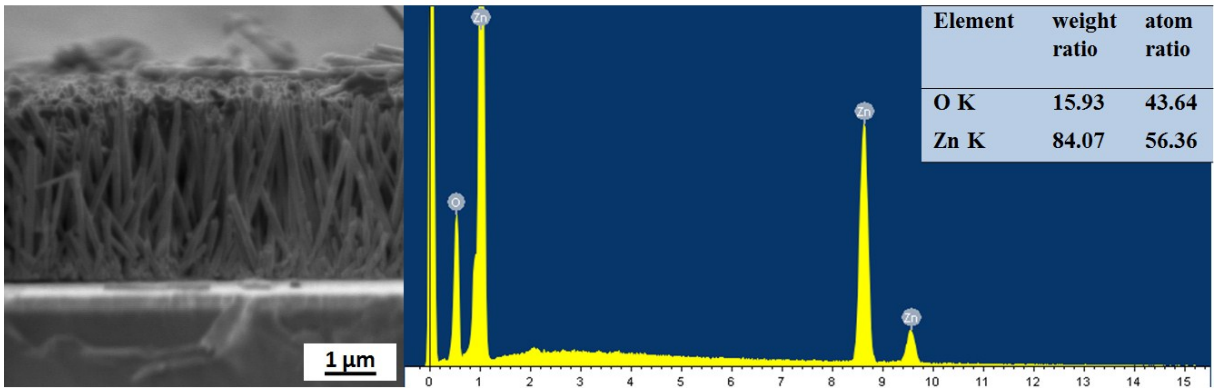

Element	weight ratio	atom ratio
O K	15.93	43.64
Zn K	84.07	56.36

Figure S1. SEM image and corresponding EDX spectrum of the ZnO arrays.

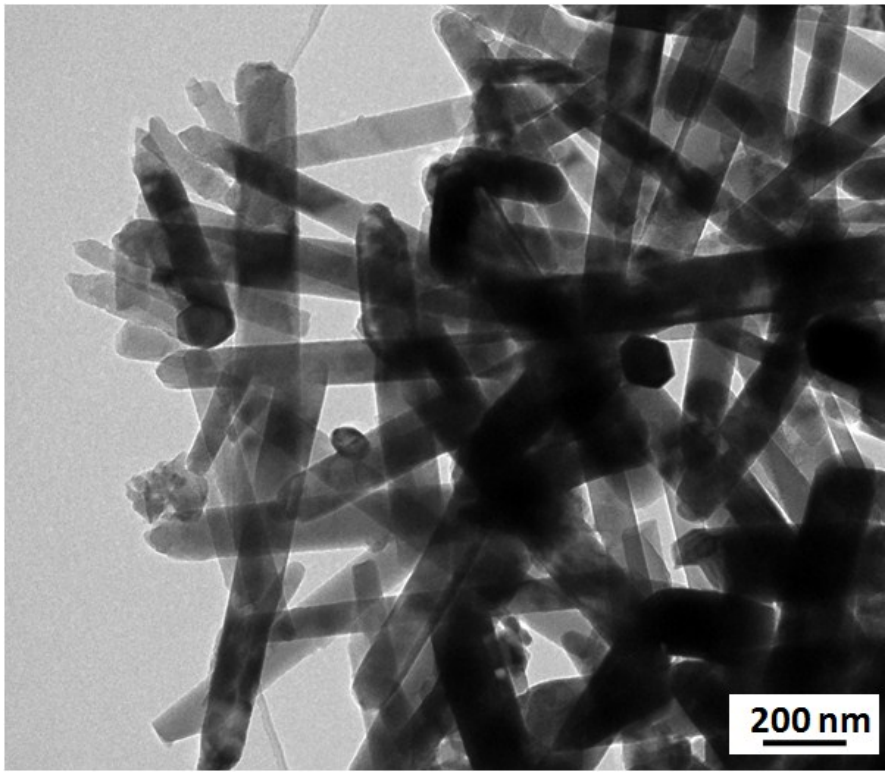

Figure S2. TEM image of the ZnO nanorods.

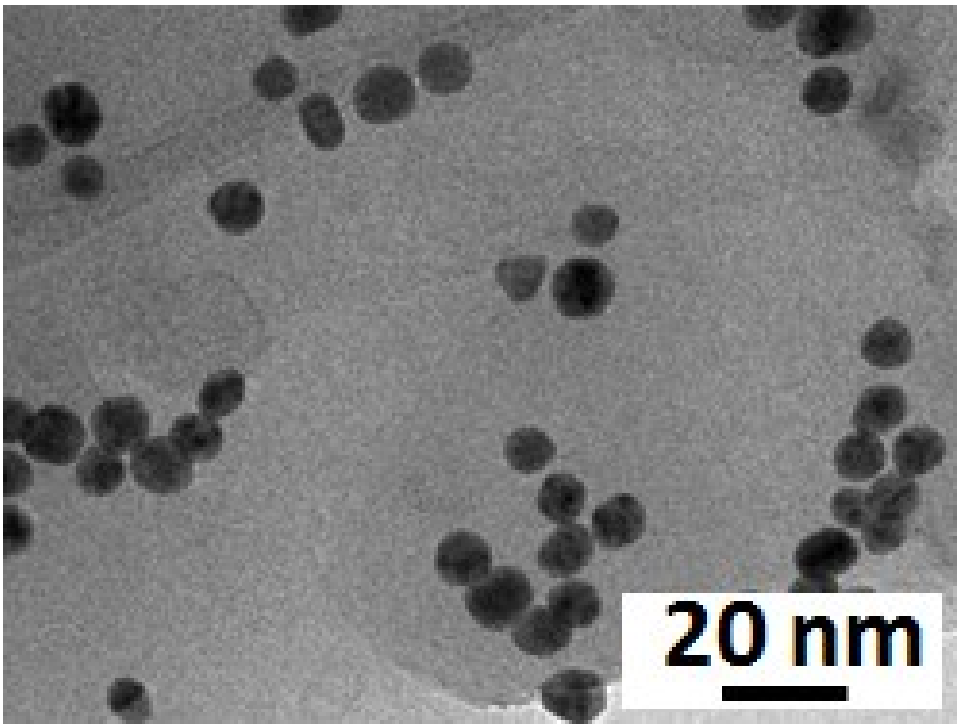

Figure S3. TEM image of the Au nanoparticles.

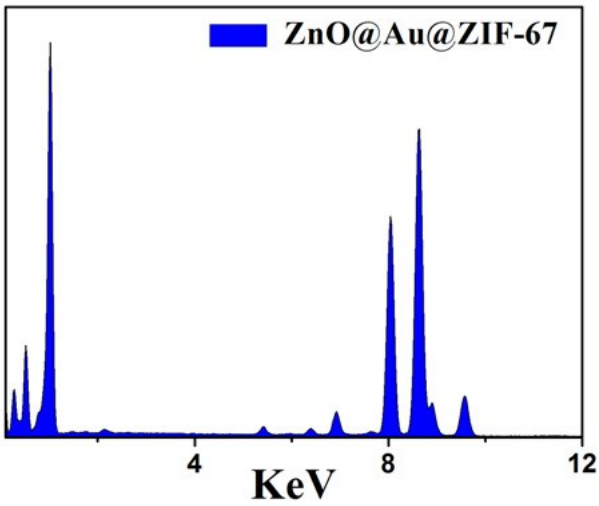

Element	Weight ratio (%)	Atom ratio (%)
Zn	93.35	93.46
Co	5.56	6.18
Au	1.08	0.36

Figure S4. EDX spectrum and corresponding elemental analysis of the ZnO@Au@ZIF-67 arrays.

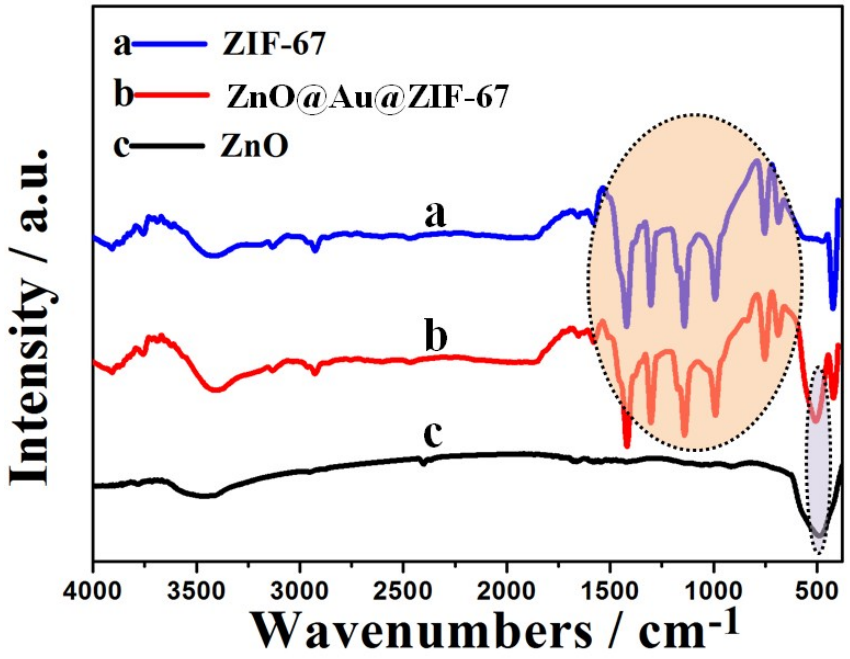

Figure S5. FT-IR spectra of ZIF-67, ZnO@Au@ZIF-67, and ZnO.

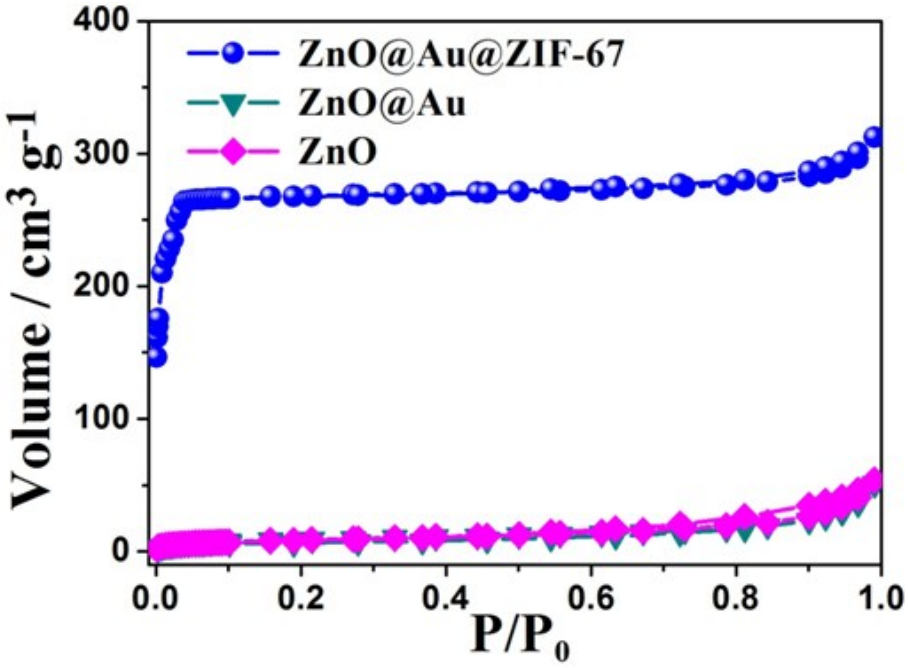

Figure S6. N_2 adsorption/desorption isotherms of ZnO, ZnO@Au, and ZnO@Au@ZIF-67.

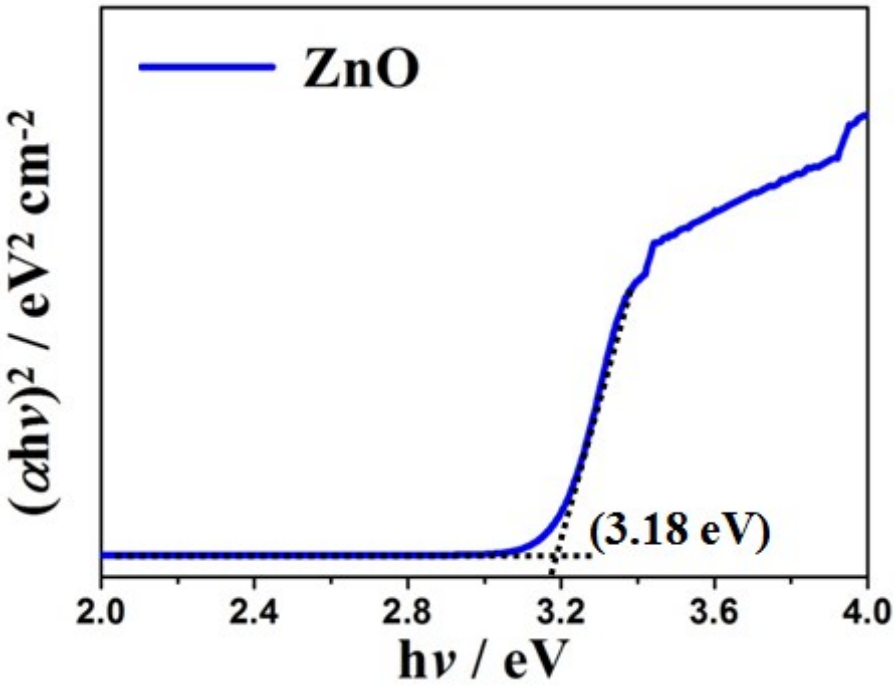

Figure S7. Plot of $(\alpha h\nu)^2$ *vs*. $h\nu$ for the ZnO nanorods corresponding to its UV-Vis diffuse reflectance spectrum for the determination of the direct bandgap.

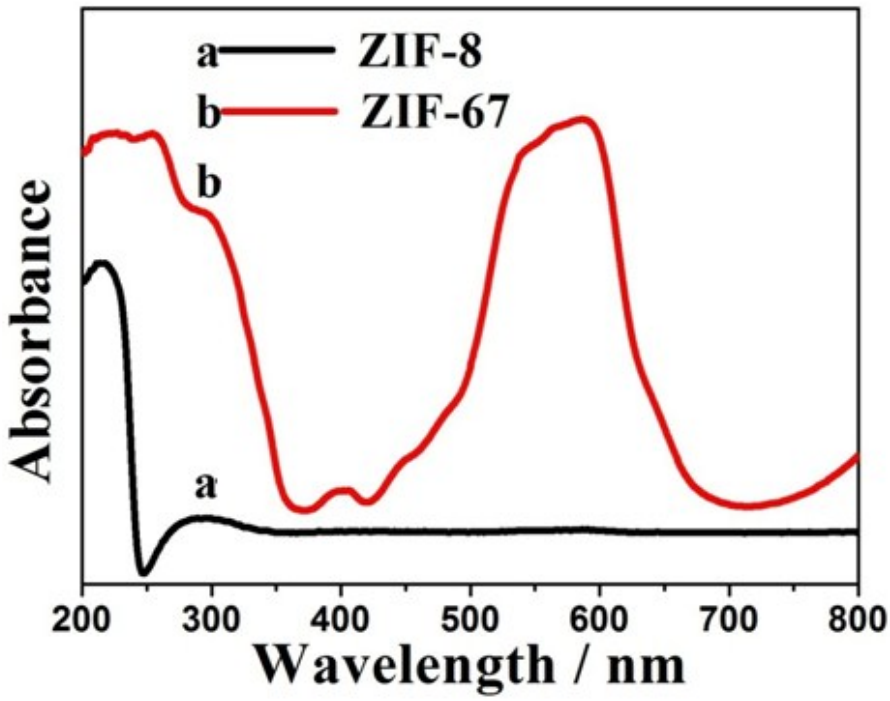

Figure S8. UV-Vis diffuse reflectance spectra of ZIF-8 and ZIF-67.

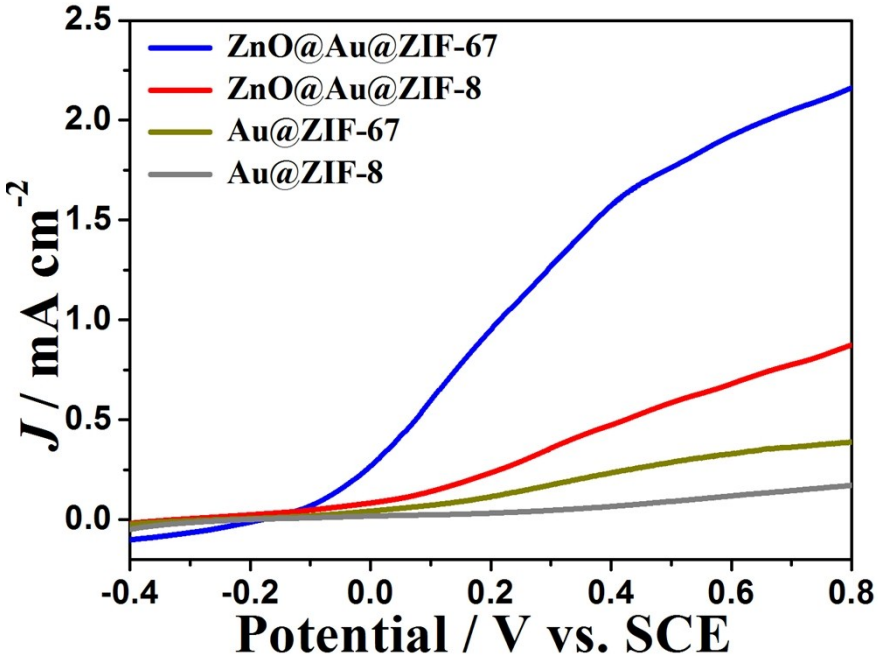

Figure S9. *J-V* curves for Au@ZIF-8, Au@ZIF-67, ZnO@Au@ZIF-8, and ZnO@Au@ZIF-67.

Table S1. A comparison of the ZnO@Au@ZIF-67 photoanode in this work with previously reported photoanodes for PEC water splitting in neutral medium.

Photoanode	Photocurrent density	Light intensity	Testing conditions	Reference
TiO_2@rGO@NiFe-LDH	1.74 mA cm^{-2} at 1.23 V *vs.* RHE	100 mW cm^{-2}	0.5 M Na_2SO_4 (pH = 6.8); 10 mV s^{-1}	*Energy Environ. Sci.* **2016**, *9*, 2633
ZnO@CoNi-LDH	~1.49 mA cm^{-2} at 1.23 V *vs.* RHE	100 mW cm^{-2}	0.5 M Na_2SO_4 (pH = 6.8); 10 mV s^{-1}	*Adv. Funct. Mater.* **2014**, *24*, 580
AZO/TiO_2/Au nanocone arrays	1.1 mA cm^{-2} at 1.23 V *vs.* RHE	100 mW cm^{-2}	0.1 M Na_2SO_4 (pH = 6.8); 10 mV s^{-1}	*Adv. Energy Mater.* **2016**, *6*, 1501496
CoO_x/$BiVO_4$	~1.75 mA cm^{-2} at 1.23 V *vs.* RHE	100 mW cm^{-2}	0.1 M KPi buffer solution (pH = 7); 10 mV s^{-1}	*J. Am. Chem. Soc.* **2015**, *137*, 5053
NiO/CoO_x/$BiVO_4$	3.50 mA cm^{-2} at 1.23 V *vs.* RHE			
Co-Pi/WO_3 NPA film	~1.95 mA cm^{-2} at 1.23 V *vs.* RHE	100 mW cm^{-2}	0.1 M Na_2SO_4; 5 mV s^{-1}	*Appl. Catal. B-Environ.* **2017**, *202*, 388
Ni-B/ZnO	1.22 mA cm^{-2} at 1.0 V *vs.* RHE	100 mW cm^{-2}	0.2 M Na_2SO_4 with 0.1 M phosphate buffer (pH = 7); 20 mV s^{-1}	*Chem. Eur. J.* **2014**, 20, 12954
Au NP/$ZnFe_2O_4$/ZnO	1.1 mA cm^{-2} at 0.8 V *vs.* Ag/AgCl	100 mW cm^{-2}	0.5 M Na_2SO_4 (pH = 6.8); 10 mV s^{-1}	*small* **2013**, *9*, 2091
ZnO (000-1) single crystal	1.84 mA cm^{-2} at 1.23 V *vs.* RHE	100 mW cm^{-2}	0.5 M Na_2SO_4; 20 mV s^{-1}	*Chem. Mater.* **2016**, *28*, 6614
3D ZnO/TiO2/FeOOH nanowire array	1.59 mA cm^{-2} at 1.80 V *vs.* RHE	100 mW cm^{-2}	0.5 M Na_2SO_4 (pH = 6.8); 20 mV s^{-1}	*Nanoscale* **2015**, *7*, 19178
Au-ZnO NR@NP	1.43 mA cm^{-2} at 1.20 V *vs.* RHE	100 mW cm^{-2}	0.5 M Na_2SO_4 (pH = 6.8); 10 mV s^{-1}	*Nano Energy* **2015**, *12*, 231
ZnO@Ag@ZIF-67	1.25 mA cm^{-2} at 1.23 V *vs.* RHE	100 mW cm^{-2}	0.5 M Na_2SO_4 (pH = 6.8); 10 mV s^{-1}	This work
ZnO@Pt@ZIF-67	1.35 mA cm^{-2} at 1.23 V *vs.* RHE	100 mW cm^{-2}	0.5 M Na_2SO_4 (pH = 6.8); 10 mV s^{-1}	This work
ZnO@Au@ZIF-67	1.93 mA cm^{-2} at 1.23 V *vs.* RHE	100 mW cm^{-2}	0.5 M Na_2SO_4 (pH = 6.8); 10 mV s^{-1}	This work

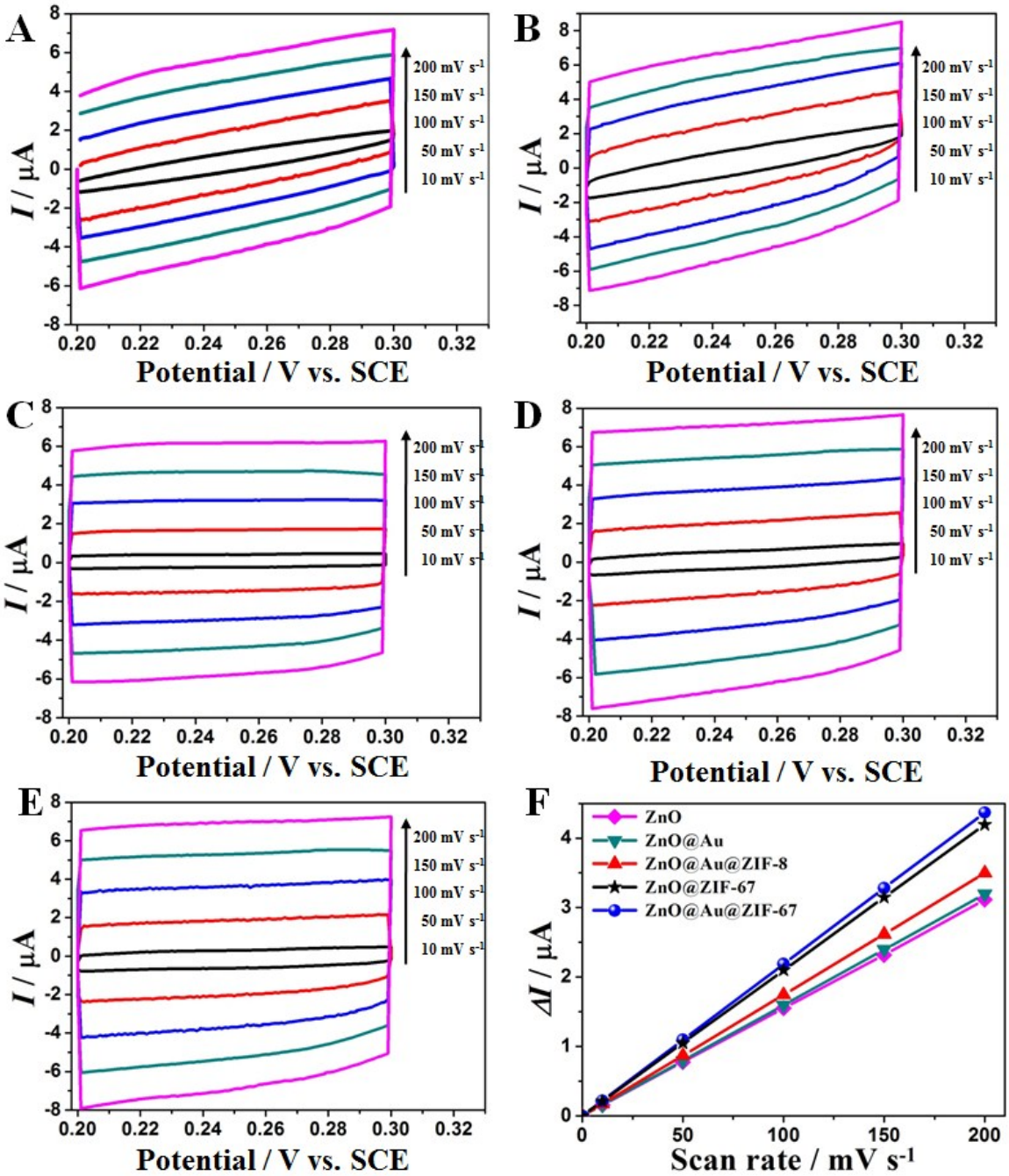

Figure S10. CV curves measured in the non-Faradaic region of 0.2−0.3 V at various scan rates for (A) ZnO, (B) ZnO@Au, (C) ZnO@Au@ZIF-8, (D) ZnO@ZIF-67, and (E) ZnO@Au@ZIF-67. (F) The double-layer capacitances (C_{dl}) of these photoanodes at a potential of 0.25 V *vs*. SCE against the scan rate.

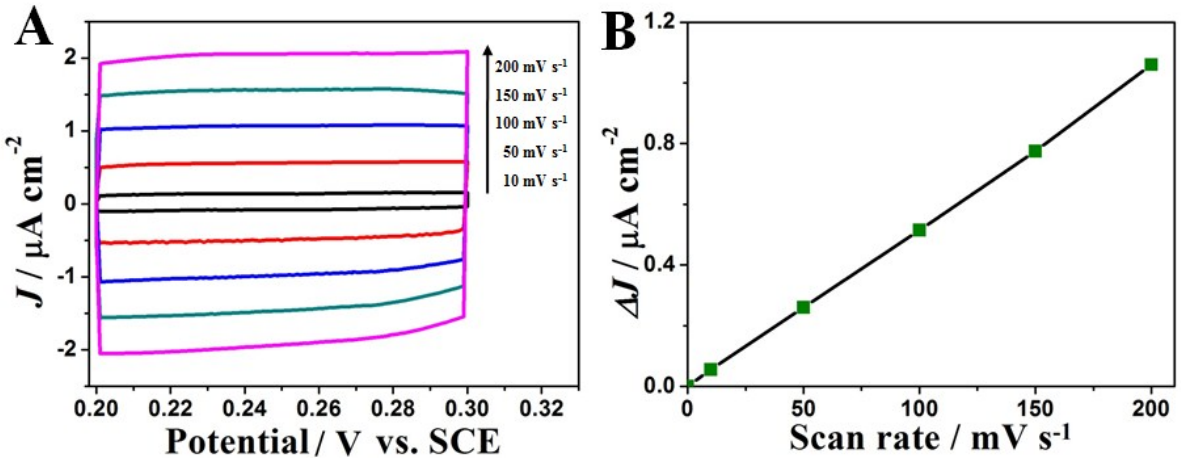

Figure S11. C_{dl} measurements for determining the specific capacitance (*Cs*) of the ITO substrate from cyclic voltammetry (CV): (A) CV curves measured in the non-Faradaic region of 0.2−0.3 V at various scan rates; (B) Charging current-density differences at a potential of 0.25 V *vs*. SCE against the scan rate.

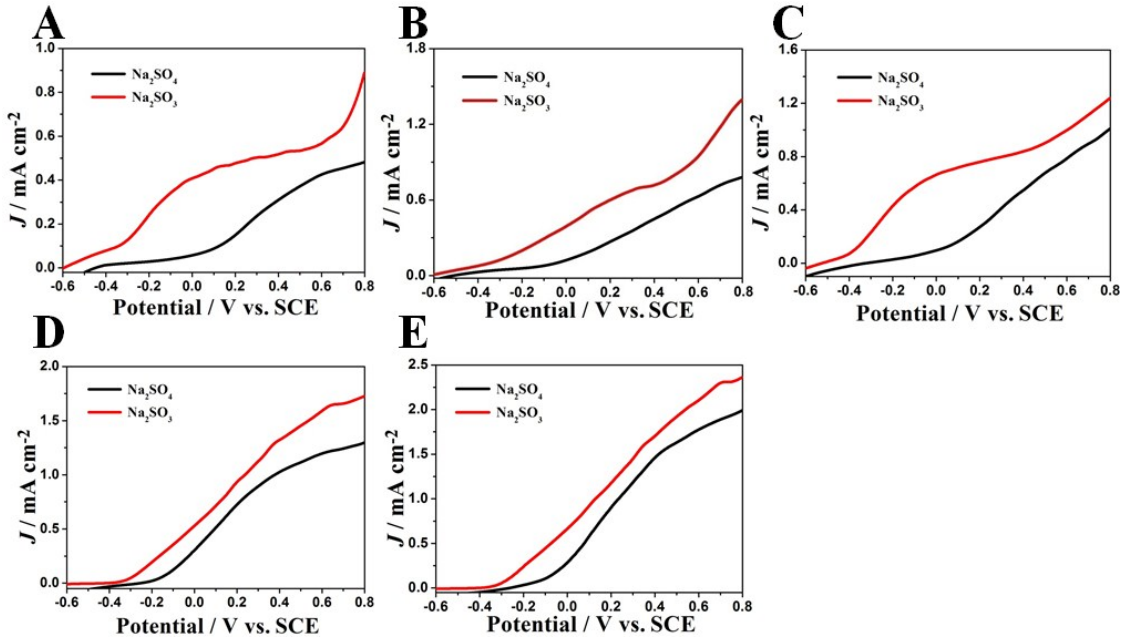

Figure S12. *J-V* curves of (A) ZnO, (B) ZnO@Au, (C) ZnO@Au@ZIF-8, (D) ZnO@ZIF-67, and (E) ZnO@Au@ZIF-67 in Na_2SO_4 and Na_2SO_3 electrolytes.

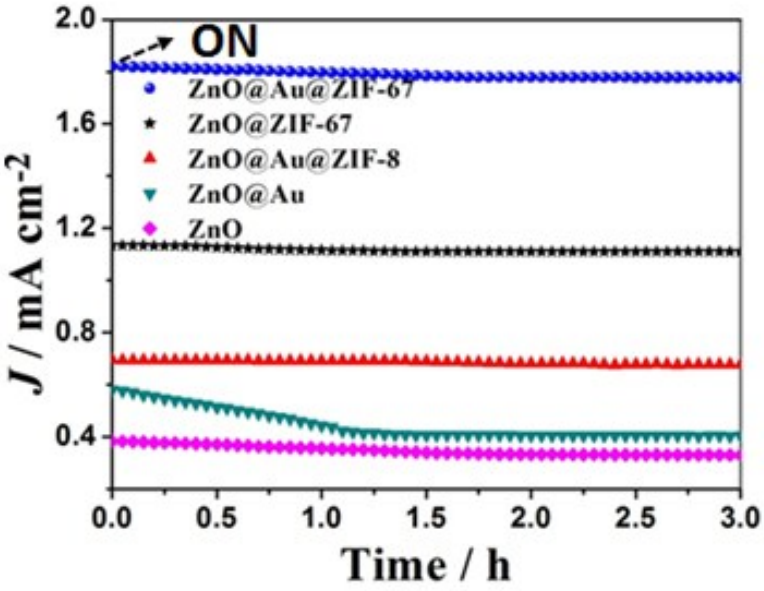

Figure S13. The photocurrent density as the function of test time for ZnO, ZnO@Au, ZnO@Au@ZIF-8, ZnO@ZIF-67, and ZnO@Au@ZIF-67.

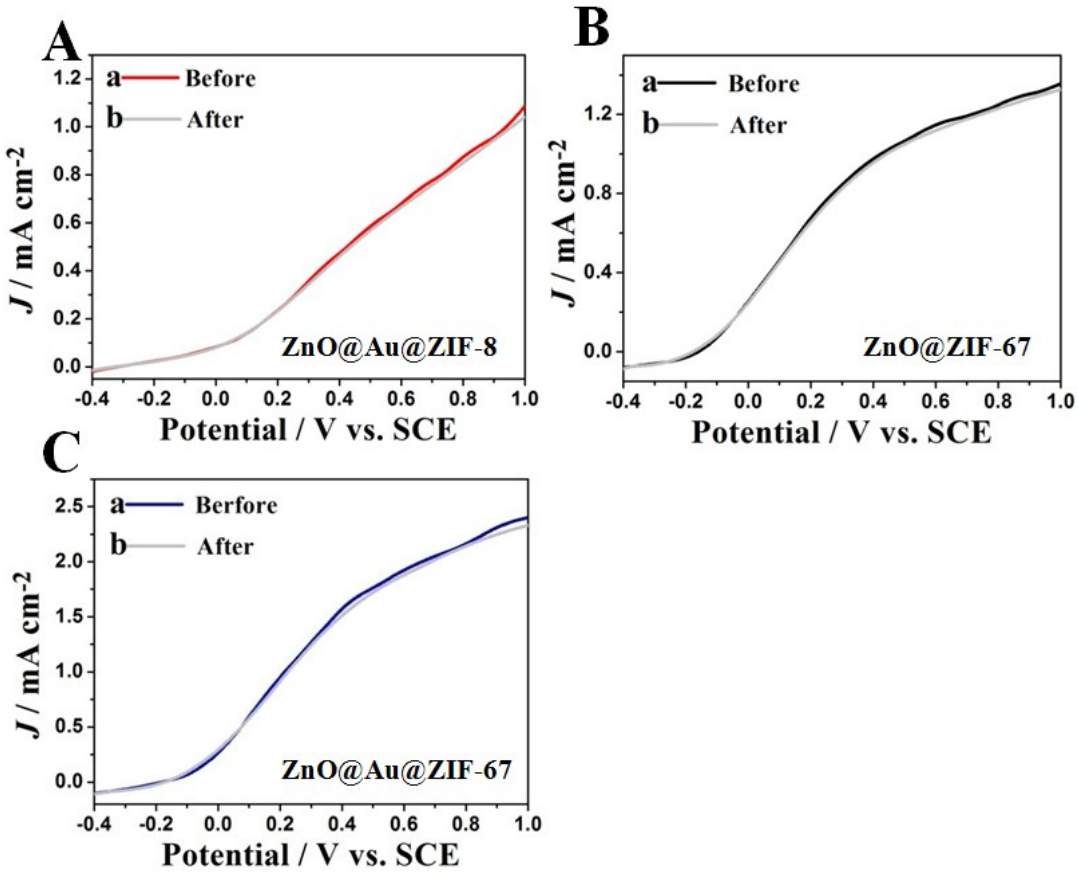

Figure S14. *J-V* curves of (A) ZnO@Au@ZIF-8, (B) ZnO@ZIF-67, and (C) ZnO@Au@ZIF-67 before and after 3-h tests.

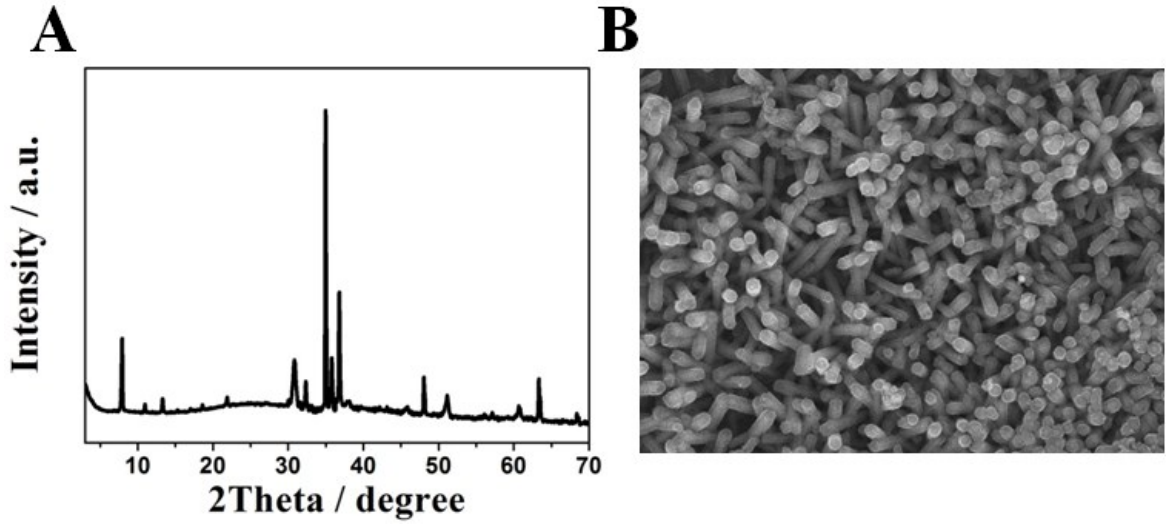

Figure S15. (A) PXRD pattern and (B) SEM image of ZnO@Au@ZIF-67 after a 3-h test.

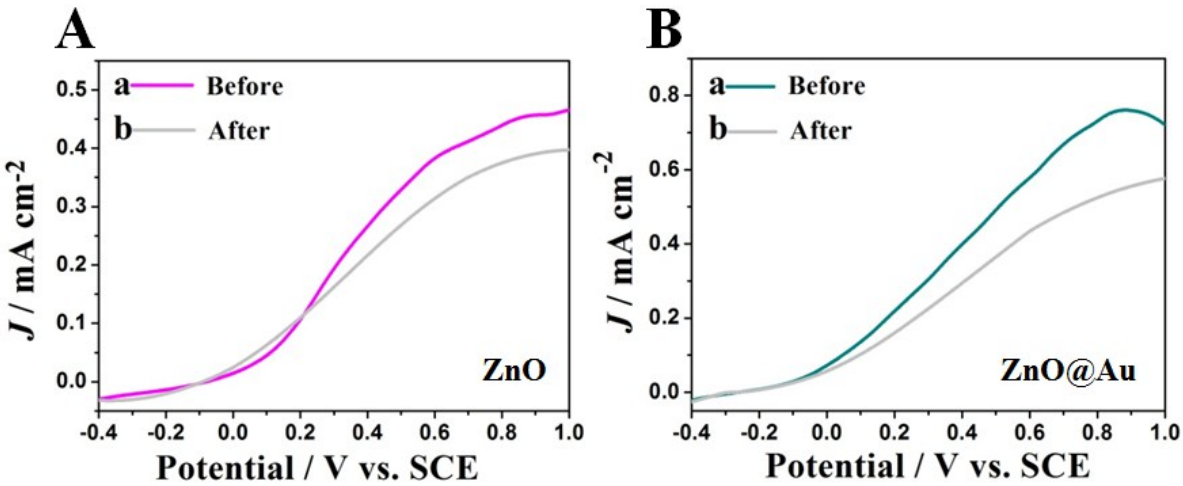

Figure S16. *J-V* curves of (A) ZnO and (B) ZnO@Au before and after a 3-h tests.

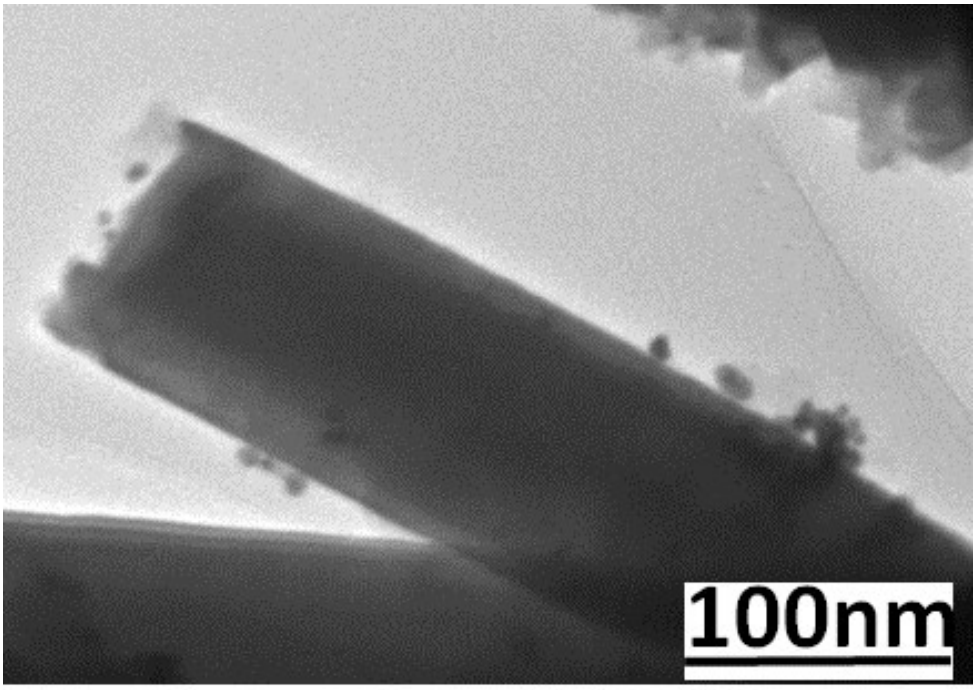

Figure S17. TEM image of ZnO@Au after a 3-h test.

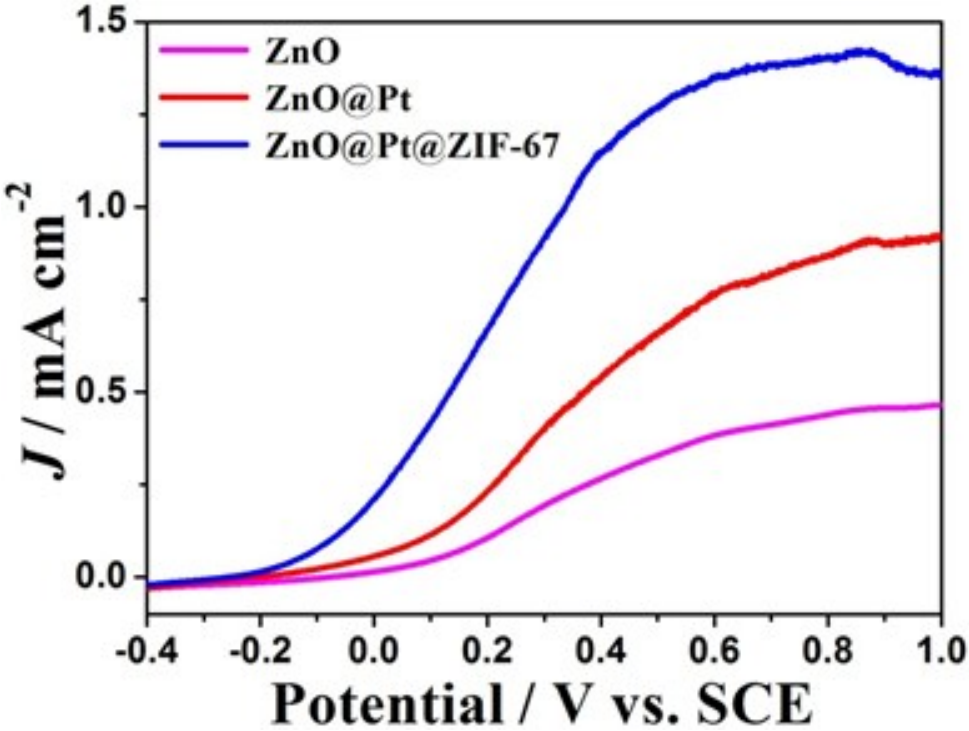

Figure S18. *J-V* curves of ZnO, ZnO@Pt, and ZnO@Pt@ZIF-67.

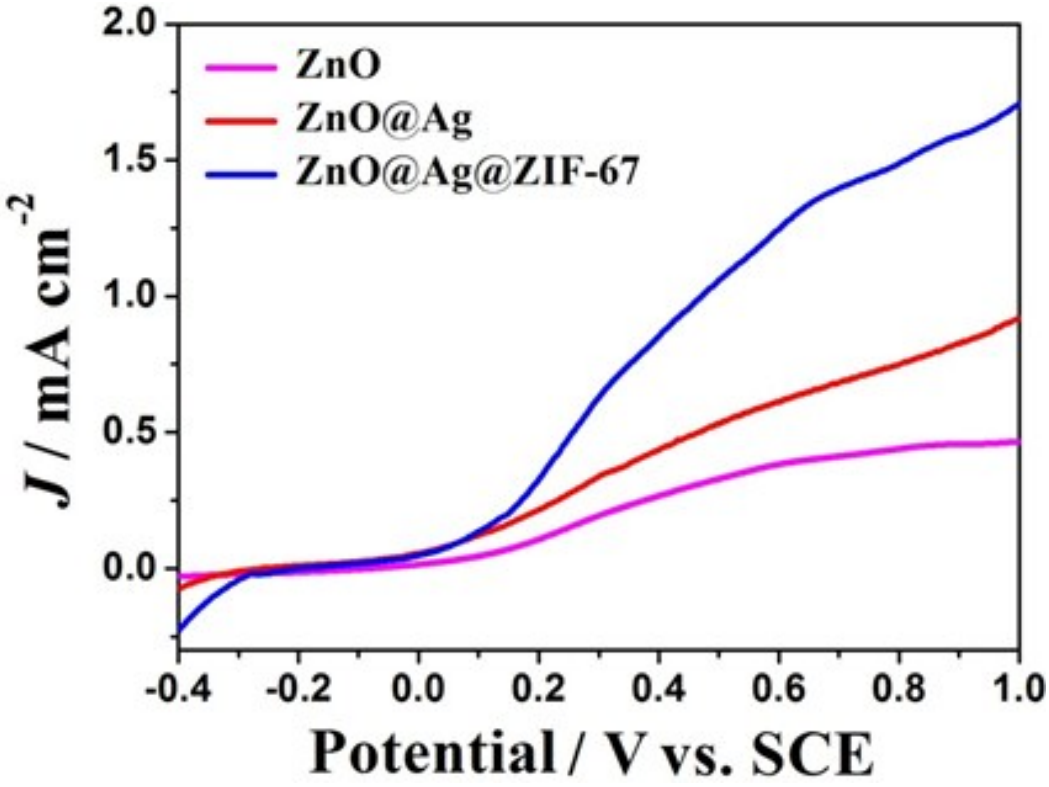

Figure S19. *J-V* curves of ZnO, ZnO@Ag, and ZnO@Ag@ZIF-67.

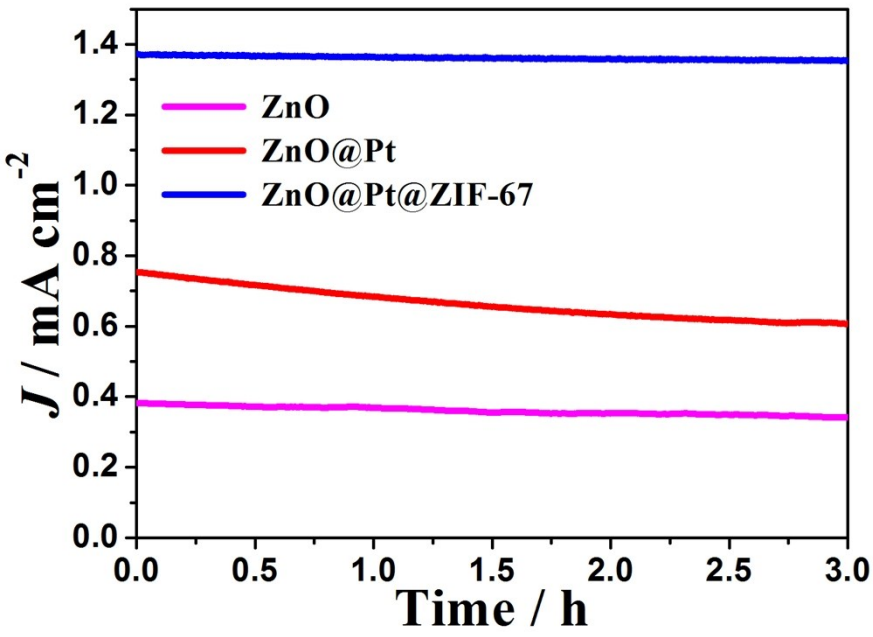

Figure S20. Photocurrent density as a function of the test time for ZnO, ZnO@Pt, and ZnO@Pt@ZIF-67.

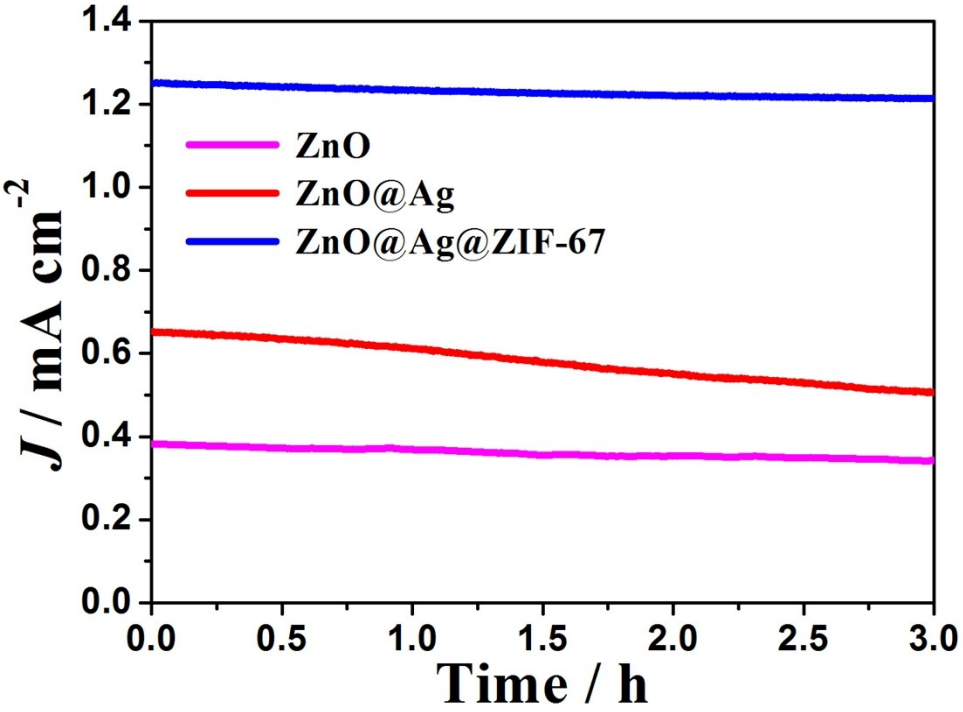

Figure S21. Photocurrent density as a function of the test time for ZnO, ZnO@Ag, and ZnO@Ag@ZIF-67.

References

1 G. Wang, X. Xiao, W. Li, Z. Lin, Z. Zhao, C. Chen, C. Wang, Y. Li, X. Huang, L. Miao, C. Jiang, Y. Huang and X. Duan, *Nano Lett*., 2015, **15**, 4692−4698.

2 P. Zhou, J. Yu and M. Jaroniec, *Adv. Mater*., 2014, **26**, 4920−4935.

3 M. Li, Z. Zhao, T. Cheng, A. Fortunelli, C.-Y. Chen, R. Yu, Q. Zhang, L. Gu, B. V. Merinov, Z. Lin, E. Zhu, T. Yu, Q. Jia, J. Guo, L. Zhang, W. A. Goddard, Y. Huang and X. Duan, *Science*, 2016, **354**, 1414−1419.

4 T. Y. Ma, S. Dai, M. Jaroniec and S. Z. Qiao, *J. Am. Chem. Soc*., 2014, **136**, 13925−13931.

5 C. C. L. McCrory, S. Jung, J. C. Peters and T. F. Jaramillo, *J. Am. Chem. Soc.*, 2013, **135**, 16977−16987.

6 Z. Wang, J. Han, Z. Li , M. Li, H. Wang, X. Zong and C. Li, *Adv. Energy Mater*., 2016, **6**, 1600864 (1−8).

7 B. Zhang, Z. Wang, B. Huang, X. Zhang, X. Qin, H. Li, Y. Dai and Y. Li, *Chem. Mater*.,

2016, **28**, 6613−6620.

8 H. Dotan, K. Sivula, M. Grätzel, A. Rothschild and S. C. Warren, *Energy Environ. Sci*., 2011, **4**, 958−964.

9 F. Ning, M. Shao, S. Xu, Y. Fu, R. Zhang, M. Wei, D. G. Evans and X. Duan, *Energy Environ. Sci*., 2016, **9**, 2633−2643.